TOXICOLOGICAL SCIENCES **139(2)**, 407–420 2014
doi: 10.1093/toxsci/kfu042
Advance Access publication March 4, 2014

The Mixture of "Ecstasy" and Its Metabolites Impairs Mitochondrial Fusion/Fission Equilibrium and Trafficking in Hippocampal Neurons, at *In Vivo* Relevant Concentrations

Daniel José Barbosa,[*,†,1] Romàn Serrat,[†,1] Serena Mirra,[†] Martí Quevedo,[†] Elena Goméz de Barreda,[‡] Jesús Àvila,[‡] Luísa Maria Ferreira,[§] Paula Sério Branco,[§] Eduarda Fernandes,[¶] Maria de Lourdes Bastos,[*] João Paulo Capela,[*,‖] Eduardo Soriano,[†,2] and Félix Carvalho[*,2,3]

**REQUIMTE (Rede de Química e Tecnologia), Toxicology Laboratory, Department of Biological Sciences, Faculty of Pharmacy, University of Porto, Rua Jorge Viterbo Ferreira 228, 4050-313 Porto, Portugal; †Centro de Investigación Biomédica en Red sobre Enfermedades Neurodegenerativas (CIBERNED, ISCIII); Department of Cell Biology, Faculty of Biology, University of Barcelona; Developmental Neurobiology and Regeneration Lab, Institute for Research in Biomedicine, Barcelona Science Park, C/Baldiri Reixac 10-12, 08028 Barcelona, Spain; ‡Centro de Investigación Biomédica en Red sobre Enfermedades Neurodegenerativas (CIBERNED, ISCIII); Center of Molecular Biology Severo Ochoa (CSIC-UAM), C/Nicolás Cabrera 1, Campus de la Universidad Autónoma de Madrid, 28049 Madrid, Spain; §REQUIMTE, CQFB (Centro de Química Fina e Biotecnologia), Chemistry Department, Faculty of Science and Technology, New University of Lisbon, 2829-516 Caparica, Portugal; ¶REQUIMTE, Laboratory of Applied Chemistry, Department of Chemical Sciences, Faculty of Pharmacy, University of Porto, Rua Jorge Viterbo Ferreira 228, 4050-313 Porto, Portugal; and ‖Faculty of Health Sciences, University Fernando Pessoa, Rua 9 de Abril 349, 4249-004 Porto, Portugal*

[1]These authors contributed equally to this study.
[2]F.C. and E.S. are co-senior authors.
[3]To whom correspondence should be addressed. Fax: +351 226 093 390. E-mail: felixdc@ff.up.pt.

Received January 17, 2014; accepted February 20, 2014

3,4-Methylenedioxymethamphetamine (MDMA; "ecstasy") is a potentially neurotoxic recreational drug of abuse. Though the mechanisms involved are still not completely understood, formation of reactive metabolites and mitochondrial dysfunction contribute to MDMA-related neurotoxicity. Neuronal mitochondrial trafficking, and their targeting to synapses, is essential for proper neuronal function and survival, rendering neurons particularly vulnerable to mitochondrial dysfunction. Indeed, MDMA-associated disruption of Ca^{2+} homeostasis and ATP depletion have been described in neurons, thus suggesting possible MDMA interference on mitochondrial dynamics. In this study, we performed real-time functional experiments of mitochondrial trafficking to explore the role of *in situ* mitochondrial dysfunction in MDMA's neurotoxic actions. We show that the mixture of MDMA and six of its major *in vivo* metabolites, each compound at 10μM, impaired mitochondrial trafficking and increased the fragmentation of axonal mitochondria in cultured hippocampal neurons. Furthermore, the overexpression of mitofusin 2 (Mfn2) or dynamin-related protein 1 (Drp1) K38A constructs almost completely rescued the trafficking deficits caused by this mixture. Finally, in hippocampal neurons overexpressing a Mfn2 mutant, Mfn2 R94Q, with impaired fusion and transport properties, it was confirmed that a dysregulation of mitochondrial fission/fusion events greatly contributed to the reported trafficking phenotype. In conclusion, our study demonstrated, for the first time, that the mixture of MDMA and its metabolites, at concentrations relevant to the *in vivo* scenario, impaired mitochondrial trafficking and increased mitochondrial fragmentation in hippocampal neurons, thus providing a new insight in the context of "ecstasy"-induced neuronal injury.

Key words: **3,4-methylenedioxymethamphetamine (MDMA; "ecstasy"); MDMA's metabolites; mitochondrial dysfunction; mitochondrial fusion/fission; mitochondrial trafficking; neurotoxicity.**

3,4-Methylenedioxymethamphetamine (MDMA; "ecstasy") is a worldwide major drug of abuse with well-documented neurotoxic properties, both in humans (Roberts *et al.*, 2009; Tai *et al.*, 2011) and in laboratory animals (Bai *et al.*, 2001; Granado *et al.*, 2011). Though the molecular and cellular mechanisms underlying MDMA's neurotoxicity remain poorly understood, recent studies have attributed a possible role to mitochondrial-dependent pathways (Alves *et al.*, 2007, 2009a,b; Puerta *et al.*, 2010; Quinton and Yamamoto, 2006). Hepatic formation of reactive metabolites, followed by their uptake into the brain (Erives *et al.*, 2008; Jones *et al.*, 2005), has also been postulated to contribute to MDMA-related neurotoxicity (Barbosa *et al.*, 2012, 2014a,b; Capela *et al.*, 2006, 2007, 2009), though their role in MDMA-induced mitochondrial dysfunction is unknown. Furthermore, mitochondrial effects of the mixture of MDMA and its major metabolites, as it occurs *in vivo*, remain uncharacterized. In fact, one of the most important limitations of *in vitro* neuronal models is the lack of cytochrome P450 (CYP450)-mediated drug's metabolism (Ferguson and Tyndale, 2011), which implies that the coexposure to parent compound and its metabolites is rarely tested (Barbosa *et al.*, 2014b).

The hepatic metabolism of MDMA is mainly regulated by CYP450 enzymes, originating 3,4-

© The Author 2014. Published by Oxford University Press on behalf of the Society of Toxicology.
All rights reserved. For permissions, please email: journals.permissions@oup.com

Downloaded from https://academic.oup.com/toxsci/article/139/2/407/2510934 by Consejo Superior de Investigaciones Cientificas (CSIC) user on 19 October 2021

methylenedioxyamphetamine (MDA) by *N*-demethylation. Both MDMA and MDA are then *O*-demethylenated to the catecholic compounds *N*-methyl-α-methyldopamine (N-Me-α-MeDA) and α-methyldopamine (α-MeDA), respectively, which can undergo oxidation to the correspondent redox-active *ortho*-quinones (Pizarro *et al.*, 2004). These *ortho*-quinones may be conjugated with reduced glutathione (GSH), originating glutathionyl adducts (Erives *et al.*, 2008). The systemic formation of 5-(glutathion-*S*-yl)-*N*-methyl-α-methyldopamine [5-(GSH)-N-Me-α-MeDA] and 5-(glutathion-*S*-yl)-α-methyldopamine [5-(GSH)-α-MeDA] is followed by their uptake into the brain (Erives *et al.*, 2008; Jones *et al.*, 2005), where they may undergo further metabolism to *N*-acetyl-cysteine (NAC) conjugates, which are slowly eliminated, and, consequently, persistent in the brain (Jones *et al.*, 2005). Supporting a role for metabolism in MDMA-induced neurotoxicity, Gollamudi *et al.* (1989) showed an attenuation of MDMA-mediated 5-HT deficits after inhibition of CYP450-mediated MDMA's metabolism. Therefore, it is expected that MDMA's neurotoxic actions may result from a combined effect between parent compound and its metabolites, as they coexist in the brain (Chu *et al.*, 1996; Erives *et al.*, 2008; Jones *et al.*, 2005; Mueller *et al.*, 2009). However, the mechanistic studies performed *in vitro* frequently investigate each compound alone, which excludes the contribution of the mixture of MDMA and its metabolites encountered *in vivo*. Notably, we previously demonstrated that the mixture of MDMA and its metabolites, at *in vivo* relevant concentrations (Chu *et al.*, 1996; Erives *et al.*, 2008; Jones *et al.*, 2005), triggered cellular adaptations and toxicity in human SH-SY5Y differentiated cells, which provided a new breakthrough in the context of MDMA-induced neurotoxicity (Barbosa *et al.*, 2014b).

Mitochondria are highly dynamic organelles that, by undergoing fission and fusion events, can display significant variability in their size and shape. In neurons, these opposing processes appear to play a key role in regulating mitochondrial distribution along axons and dendrites, rendering neuronal cells critically dependent on mitochondrial dynamics (Sheng and Cai, 2012). Mitochondrial fission is mediated by an evolutionarily conserved soluble cytosolic dynamin-related guanosine 5′-triphosphatase (GTPase) protein, the dynamin-related protein 1 (Drp1), whose interaction with mitochondria is regulated by posttranslational modifications (Itoh *et al.*, 2013) and Ca^{2+} (Cereghetti *et al.*, 2008). Mitochondrial fusion is mediated by the dynamin-related GTPase proteins, mitofusin 1 (Mfn1), mitofusin 2 (Mfn2), and optic dominant atrophy 1 (Opa1) (Itoh *et al.*, 2013). Whereas Mfn1 and Mfn2 are involved in the outer mitochondrial membrane fusion, Opa1 mediates fusion of the inner membrane (Song *et al.*, 2009). A disruption of this dynamic equilibrium between mitochondrial fusion and fission may herald neuronal injury or death and contribute to the development of neurodegenerative disorders (Wang *et al.*, 2013a).

Axonal transport of mitochondria along microtubules is mediated by motor proteins, kinesins, and dyneins. In axons, kinesins, linked to the outer mitochondrial membrane protein Miro, through the adaptor proteins Milton/Trak, mediate anterograde transport, whereas cytoplasmic dyneins mediate retrograde transport (MacAskill and Kittler, 2010). Additionally, motor proteins' function is highly regulated by Ca^{2+} (Macaskill *et al.*, 2009; Wang and Schwarz, 2009) and critically dependent on ATP locally produced by mitochondria (Sheng and Cai, 2012). In Drosophila neurons, a Miro-dependent regulation of retrograde axonal transport of mitochondria was also described (Russo *et al.*, 2009). Microtubule-associated protein Tau, by assembly and maintenance of microtubules, also plays a major role in neuronal mitochondrial trafficking control (Kopeikina *et al.*, 2011; Llorens-Martín *et al.*, 2011; Vossel *et al.*, 2010). Tau function is largely dependent on its phosphorylation status (Llorens-Martín *et al.*, 2011; Shahpasand *et al.*, 2012). Notably, MDMA was reported to raise intracellular free Ca^{2+} levels in cultured hippocampal neurons (Barbosa *et al.*, 2014c), and also to increase Tau's phosphorylation in both mouse hippocampus (Busceti *et al.*, 2008) and cultured hippocampal neurons (Barbosa *et al.*, 2014c), thus suggesting a possible direct interference of MDMA on mitochondrial dynamics.

By controlling organelle size, mitochondrial fission/fusion events also regulate an efficient microtubule-mediated active transport in neurons (Itoh *et al.*, 2013). Accordingly, Mfn2 was recently described as necessary for neuronal mitochondrial transport, by interacting with the Miro/Milton complex (Misko *et al.*, 2010). Also, a Drp1-dependent regulation of mitochondrial density in dendrites (Li *et al.*, 2004) and a prevention of axonal transport of mitochondria in the absence of fission events (Verstreken *et al.*, 2005) were reported, illustrating the interplay between mitochondrial fission/fusion events and movement.

Considering that MDMA and its metabolites coexist in the brain, our hypothesis is that their mixture, at a range of concentrations relevant to the *in vivo* scenario, may dysregulate mitochondrial dynamics. To this end, by using real-time fluorescence video-microscopy at single-cell resolution, we evaluated the putative disrupting effects of the mixture of MDMA and its metabolites on mitochondrial fusion/fission and trafficking.

MATERIALS AND METHODS

Materials. All reagents used were of analytical grade or of the highest grade available. Neurobasal medium, B27 supplement, penicillin/streptomycin 10,000 U/ml, GlutaMAX™ supplement, 0.5% trypsin/ethylenediaminetetraacetic acid (EDTA) without phenol red, heat inactivated horse serum, Opti-MEM medium, Lipofectamine 2000 and Dulbecco's phosphate buffered saline (DPBS) were purchased from Gibco Laboratories (Lenexa, KS). Poly-L-lysine (PLL), triton X-100, Na_3VO_4, NaF, Tris·HCl, bromophenol blue, β-mercaptoethanol and 3-(4,5-dimethyl-2-thiazolyl)-2,5-diphenyl-2H-tetrazolium

Downloaded from https://academic.oup.com/toxsci/article/139/2/407/2510934 by Consejo Superior de Investigaciones Cientificas (CSIC) user on 19 October 2021

(MTT) bromide were obtained from Sigma-Aldrich (St Louis, MO). DNAse recombinant I and complete protease's inhibitor cocktail were obtained from Roche Diagnostics (Mannheim, Germany). Mouse anti-Tau-1 and mouse anti-α-actin monoclonal antibodies were purchased from Merck Millipore (Merck KGaA, Darmstadt, Germany). Goat antimouse IgG-peroxidase polyclonal antibody was purchased from DAKO (Glostrup, Denmark). MDMA (hydrochloride salt) was extracted and purified from high purity MDMA tablets kindly provided by the Portuguese Criminal Police Department. The obtained salt was pure and fully characterized by NMR and mass spectrometry methodologies. MDMA's metabolites α-MeDA, N-Me-α-MeDA, 5-(GSH)-α-MeDA, 5-(GSH)-N-Me-α-MeDA, 5-(*N*-acetylcystein-*S*-yl)-α-methyldopamine [5-(NAC)-α-MeDA], and 5-(*N*-acetylcystein-*S*-yl)-*N*-methyl-α-methyldopamine [5-(NAC)-N-Me-α-MeDA] were synthesized and fully characterized by NMR and mass spectrometry methodologies by REQUI*M*TE (Centro de Química Fina e Biotecnologia), Chemistry Department, Faculty of Sciences and Technology, New University of Lisbon, 2829-516 Caparica, Portugal, according to previously published methods (Capela *et al.*, 2006, 2007).

Animals. All procedures involving animals were approved by the Barcelona Scientific Park's Animal Experimentation Committee and were carried out in accordance with the "Guide for the Care and Use of Laboratory Animals" from the Institute for Laboratory Animal Research (Research, 2011), and the European Community Council's directive and the National Institute of Health's guidelines for the care and use of laboratory animals. Animals were allowed free access to a standard chow diet and water and maintained on a 12 h/12 h light/dark cycle under specific pathogen free conditions in the Barcelona Scientific Park's Animal Research Center. To prepare primary hippocampal cultures, OF1 embryos from mice (Charles River, France) and C57BL/6 Tau (−/−) mice's embryos were used, at embryonic day 15 (E15) to E16, considering the mating day as E0. All procedures were taken to minimize the number of animals used and their suffering.

Cell culture and transfection. Primary neuronal cultures of hippocampus were prepared according to previously published methods (Barbosa *et al*., 2014c). Pregnant mice were killed by cervical dislocation, and embryos were placed in ice-cold DPBS without Ca^{2+} and Mg^{2+} [DPBS (−/−)] containing 0.6% glucose during all dissection procedures. After brain isolation, meninges were removed, and hippocampus was dissected. Following a trypsinization (0.05% trypsin/EDTA) for 10 min, at 37°C, a DNAse I treatment was applied, followed by another incubation period of 10 min, again at 37°C. After dissociation of the tissue pieces by gently sweeping, cellular suspension was centrifuged at 127× g, for 5 min, at 4°C, and resuspended in complete medium (neurobasal medium supplemented with 2% B27, 100 U/ml penicillin, 100 μg/ml streptomycin, and 2mM Glutamax™). Cells were then seeded at a density of 78,000 cells/cm^2. For live-imaging, hippocampal cultures were seeded in precoated 35 mm *Fluordish* plates (World Precision Instruments, Florida), whereas for western blotting analysis, precoated six-well plates (Nunc, Roskilde, Denmark), were used. To evaluate mitochondrial length, hippocampal cultures were seeded in 12 mm round precoated glass coverslips. Precoating was performed by overnight incubation, at 37°C, with 0.2 mg/ml PLL solution (prepared in 0.1M borate buffer, pH 8.5). Cultures were maintained at 37°C, in an atmosphere of 5% CO_2/95% air and used for experiments at 5 days *in vitro* (DIV). Hippocampal cultures were transfected, at 4DIV, with DNA-encoding plasmids MitDsRed (a gift from Antonio Zorzano) and green fluorescent protein (GFP), or cotransfected with another of the following constructs: Mfn2 (Misko *et al.*, 2010), Mfn2 R94Q (Misko *et al.*, 2012), or Drp1 K38A (Zhao *et al.*, 2011), using Lipofectamine 2000 as transfection reagent and following the manufacturer's instructions.

Study design. Hippocampal neuronal cultures were incubated with the mixture of MDMA and its six metabolites α-MeDA, N-Me-α-MeDA, 5-(GSH)-α-MeDA, 5-(GSH)-N-Me-α-MeDA, 5-(NAC)-α-MeDA, and 5-(NAC)-N-Me-α-MeDA, each compound at 10μM, at 5DIV, and functional or biochemical experiments were performed at 6DIV (24 h of exposure).

In humans, as in rats, MDMA undergoes a nonlinear pharmacokinetics, in which its brain concentration increases nonlinearly with the dose (Baumann et al., 2009; Concheiro et al., 2014; De La Torre et al., 2000). Furthermore, in the rat model, high doses of MDMA (up to 10 mg/kg) were described to saturate hepatic metabolism, via enzymatic inhibition, thus slowing the rate of *N*-demethylation (Baumann et al., 2009; Concheiro et al., 2014; De La Torre et al., 2000). Additionally, *in vitro* studies suggest that MDMA can act as inhibitor of the cytochrome P450 (CYP) 2D6 isoenzyme, which is important for the N-Me-α-MeDA formation. This effect is likely to result from a competitive interaction and/or formation of a metabolic intermediate complex between MDMA and this enzyme (Delaforge et al., 1999; Heydari et al., 2004), though it lacks *in vivo* confirmation. Nevertheless, in a human controlled study, following a single 100 mg oral dose of MDMA, N-Me-α-MeDA reached plasma concentrations similar to those observed for MDMA (154.5 μg/l vs. 181.6 μg/l, respectively; Segura et al., 2001), clearly demonstrating a high formation rate for this catecholic metabolite.

Following oral administration of MDMA (20 mg/kg) to rats, high concentrations of MDMA were found in the brain (17.17 nmol/g brain) (Mueller et al., 2009). Similarly, after subcutaneous injection (from 5 to 20 mg/kg), brain concentrations of MDMA ranged from 0.74 to 147.65 nmol/g brain, and plasma concentrations reached 15.78μM (Chu et al., 1996), showing, therefore, that the brain accumulation of MDMA is clearly favored. Furthermore, it was also shown the presence of MDMA catecholic metabolites (Chu et al., 1996) and their correspondent GSH and NAC conjugates (Erives et al., 2008; Jones et

Downloaded from https://academic.oup.com/toxsci/article/139/2/407/2510934 by Consejo Superior de Investigaciones Cientificas (CSIC) user on 19 October 2021

al., 2005) in the brain following subcutaneous administration of MDMA (20-40 mg/kg) to rats, clearly demonstrating the compounds' ability to cross the blood-brain barrier. Interestingly, the combined concentration of the four thioether metabolites in the rat brain striatal dialysate reached the concentration of 13μM, which remained relatively unchanged for approximately 4 h after exposure to MDMA (4 × 20 mg/kg subcutaneous, at 12-h interval; Erives et al., 2008). Additionally, it is important to consider that NAC-conjugated metabolites of MDMA are formed in the brain (Esteban et al., 2001) and, therefore, the blood-brain barrier does not interfere with their brain bioavailability. This indicates that MDMA and metabolites may reach brain concentrations even higher than the ones used in our mixture composition. Thus, it is feasible to consider our mixture concentration and composition a relevant model to the *in vivo* scenario.

Live-imaging of axonal transport of mitochondria in hippocampal neurons. Live-imaging of axonal transport of mitochondria in hippocampal neurons was performed using an Olympus IX81 confocal microscope (Olympus Corporation, Tokyo, Japan), equipped with a 60x immersion objective, and an Andor Revolution XD spinning disk confocal microscopy system composed of a iXonEM + EM-CCD camera (Andor Tecnology, Belfast, United Kingdom) and FRAPPA, and solid-state laser combiner (ALC-UVP 350i, Andor Tecnology) with the renowned CSU-X1 confocal scanner (Yokogawa Electric Corporation, Tokyo, Japan). All cultures were kept at 37°C, using a heating insert on the microscope stage and an incubating chamber, allowing circulation of a control CO_2 (5%)–air heated mixture for pH control. For measurements of axonal transport of mitochondria, axonal processes in transfected hippocampal neurons were identified following morphological criteria, and directionally determined for each axon. Time-lapse series of image stacks composed of 151 images (512 × 512 pixels) were taken every 6 s, over the course of 15 min. All 151 images obtained were processed mainly with Andor IQ2 software (Andor Technology). Further images' processing and analysis and videos' compilation and edition was done with FIJI (Image JA v1.45b, Open source software, NIH). Kymographs were generated with MetaMorph Software (Molecular Devices - MDS Analytical Technologies, Sunnyvale, CA). In our presentation of kymographs, the vertical axis represents the time, and the horizontal axis is the distance along a slice. Stationary mitochondrial sites are identified as vertical lines on the kymographs. Motile mitochondria appear as diagonal lines, and their slopes provide the velocity. Distances and speeds of anterograde (from proximal to distal) and retrograde (from distal to proximal) motile mitochondria were measured separately from the corresponding kymographs. In all cases, a mitochondrion was considered motile when it moved more than 5 μm during the 15 min of recording. Mitochondrion motile in both anterograde and retrograde directions was considered a single mitochondrion, although it was included in both anterograde and retrograde moving mitochondria groups. For qualitative imaging of axonal transport of mitochondria, MitDsRed and GFP were excited at 561 and 488 nm and fluorescence emission was collected at 592 and 508 nm, respectively.

Western blotting analysis of Tau protein. Cellular proteins were extracted with lysis buffer [50mM Tris·HCl pH 7.5, 150mM NaCl, 5mM EDTA, 1% triton X-100 (vol/vol), 10% glycerol (vol/vol), complete protease's inhibitor cocktail, 1mM Na_3VO_4, 10mM $Na_4P_2O_7$, and 10mM NaF], followed by an incubation on ice for 30 min. After centrifugation at 16,000 × g, for 10 min, at 4°C, a SDS-PAGE reducing buffer [150mM Tris·HCl pH 6.8, 3% SDS (wt/vol), 30% glycerol (vol/vol), 0.075% bromophenol blue (wt/vol) and 15% β-mercaptoethanol (vol/vol)] was added to the samples (1:2 ratio), which were then boiled at 90°C for 5 min. Proteins were loaded and separated in 10% SDS/polyacrylamide gels, at a constant voltage of 120 mV. Gels were transferred to nitrocellulose membranes (Whatman, Dassel, Germany) using a transfer buffer (20% methanol (vol/vol) in 20mM Tris base and 139mM glycine), at 125 mV, for 1.5 h. Membranes were then rinsed in Tris-buffered saline solution with Tween 20 [TBS-T: 10mM Tris base, 140mM NaCl and 0.1% Tween 20 (vol/vol), pH 7.4], and nonspecific sites were blocked for 1 h, at room temperature, in blocking buffer [3% bovine serum albumine (BSA) (wt/vol) in TBS-T]. Membranes were incubated with primary antibodies (overnight at 4°C): mouse monoclonal anti-Tau1 (1:50,000) or anti-α-actin (1:100,000). After washing five times (10 min each) with TBS-T membranes were then incubated with the antimouse IgG-peroxidase secondary antibody (1:2500), for 1 h, at room temperature. All antibodies were diluted in blocking buffer. Following three washes (10 min each) with TBS-T, bands were visualized using ECL chemiluminescence reagents (Amersham Pharmacia Biotech, Buckinghamshire, United Kingdom), according to the supplier`s instructions, and quantified using the Quantity One software (Bio-Rad Laboratories).

Mitochondrial length measurements. Hippocampal cultures seeded in 12 mm round precoated glass coverslips, and transfected with MitDsRed and GFP, were incubated with the mixture of MDMA and its metabolites for 24 h and then fixed in 4% paraformaldehyde, for 20 min, at room temperature. Images were acquired in a Leica TCS SP2 confocal microscope (Leica Microsystems, Mannheim, Germany), equipped with a 60x immersion objective. Stacks of images (1024 × 1024 pixels) were acquired with Leica Confocal Software (Leica Microsystems). Further image processing and analysis was done with Fiji (NIH). Mitochondria in axonal processes were visualized by mitochondrial targeted MitDsRed. Mitochondrial length was estimated individually for each mitochondrion. To identify axonal processes GFP was excited at 488 nm, and fluorescence emission was collected at 508 nm. MitDsRed was excited at 561 nm and fluorescence intensities were collected at 592 nm.

Downloaded from https://academic.oup.com/toxsci/article/139/2/407/2510934 by Consejo Superior de Investigaciones Cientificas (CSIC) user on 19 October 2021

Data analysis. Values in figures and text are presented as mean ± SEM of the indicated number of independent experiments. Each independent experiment was performed with hippocampal cultures originating from different pregnant mice. Normality of the data distribution was assessed by three tests (Kolmogorov-Smirnov, D'Agostino and Pearson omnibus and Shapiro-Wilk normality tests). In experiments with only one variable, statistical comparisons between groups were performed with one-way ANOVA, followed by Bonferroni's test for *post-hoc* evaluations, or with Mann-Whitney's test. Two-way ANOVA followed by Bonferroni's *post hoc* test was used to analyze the data from experiments with two variables. Details of the performed statistical analysis are described in each figure legend. Differences were considered to be significant at p values lower than 0.05. All analyses were performed using GraphPad Prism 6.0 for Windows (GraphPad Software, San Diego, CA).

RESULTS

The Mixture of MDMA and its Metabolites, at In Vivo *Relevant Concentrations, Impaired Axonal Transport of Mitochondria in Hippocampal Neurons*

Based on a recent study published by our laboratory, in which it was demonstrated, for the first time, that the mixture of MDMA and its metabolites, at *in vivo* relevant concentrations, elicited cellular adaptations and toxicity in human SH-SY5Y differentiated cells (Barbosa *et al.*, 2014b), two different compositions of the mixture of MDMA and its metabolites, each compound at 10μM or each compound at 20μM, were tested. Twenty four hours of exposure to the mixture of MDMA and its metabolites α-MeDA, N-Me-α-MeDA, 5-(GSH)-α-MeDA, 5-(GSH)-N-Me-α-MeDA, 5-(NAC)-α-MeDA, and 5-(NAC)-N-Me-α-MeDA, each compound at 20μM, resulted in significant toxicity to the culture, as evaluated by the MTT reduction assay (Fig. 1). Nevertheless, exposure to the 10μM mixture, for 24 h, did not cause significant toxicity to hippocampal cultures (Fig. 1). Therefore, the 10μM mixture was selected for our further functional studies.

In humans, MDMA-induced neuronal deficits have been reported in discrete areas of the brain, such as cortex, striatum, *raphe nuclei*, and hippocampus (Capela *et al.*, 2009; Carvalho *et al.*, 2012; Parrott, 2012). Mitochondrial trafficking is a key regulator process in maintaining neuronal function and survival, because mitochondria need to be distributed from cell body, where they are synthesized, to axons and dendrites, to facilitate adequate energy supply and Ca^{2+} buffering (Sheng and Cai, 2012). Therefore, by using cultured hippocampal neurons, we aimed to evaluate the putative effects of the mixture of MDMA and its metabolites, which represent a more real scenario of *in vivo* exposure to MDMA, on axonal transport of mitochondria. Control neurons exhibited prominent mitochondrial trafficking, with an average of 65% of motile mitochondria, moving in both anterograde and retrograde directions, at

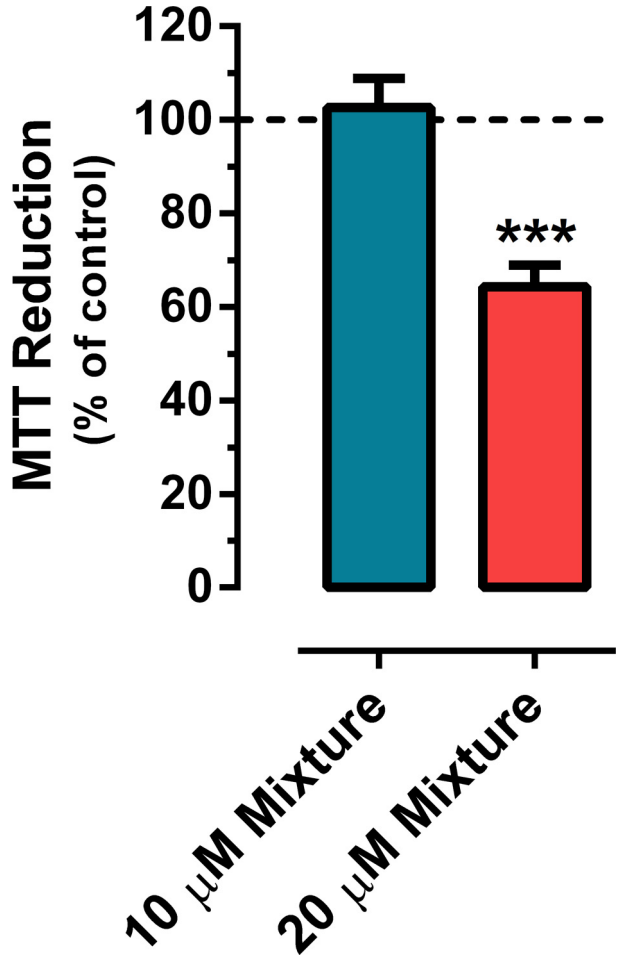

FIG. 1. Toxic effect of the mixture of MDMA and its metabolites in hippocampal cultures. After 5DIV, hippocampal cultures were exposed to the mixture of MDMA and its metabolites α-MeDA, N-Me-α-MeDA, 5-(GSH)-α-MeDA, 5-(GSH)-N-Me-α-MeDA, 5-(NAC)-α-MeDA, and 5-(NAC)-N-Me-α-MeDA, each compound at 10 or 20μM, for 24 h, and mitochondrial dysfunction was then evaluated by the MTT reduction assay. Data were analyzed using one-way ANOVA, followed by Bonferroni's test for *post-hoc* evaluations, and represent the mean ± SEM of four independent experiments (each experiment was performed in triplicate), being expressed as the percentage of the absorbance of the respective control cells [MTT reduction (% of control)] (***$p < 0.001$ mixture vs. control).

velocity of about 0.4 μm/s (Fig. 2 and Supplementary movie 1). Exposure to the mixture of MDMA and its metabolites α-MeDA, N-Me-α-MeDA, 5-(GSH)-α-MeDA, 5-(GSH)-N-Me-α-MeDA, 5-(NAC)-α-MeDA, and 5-(NAC)-N-Me-α-MeDA, each compound at 10μM, for 24 h, dramatically impaired mitochondrial neuronal trafficking (Fig. 2 and Supplementary movie 2). Analysis of the data showed a significant reduction on mitochondrial motility (control = 65.27 ± 4.89%; mixture = 42.56 ± 5.90%, $p < 0.05$), which was revealed in both anterograde (control = 43.37 ± 3.57%; mixture = 30.51 ± 4.62%, $p < 0.05$) and retrograde (control = 40.01 ± 4.61%; mixture = 24.84 ± 4.72%, $p < 0.05$) directions. Though anterograde velocity was

Downloaded from https://academic.oup.com/toxsci/article/139/2/407/2510934 by Consejo Superior de Investigaciones Cientificas (CSIC) user on 19 October 2021

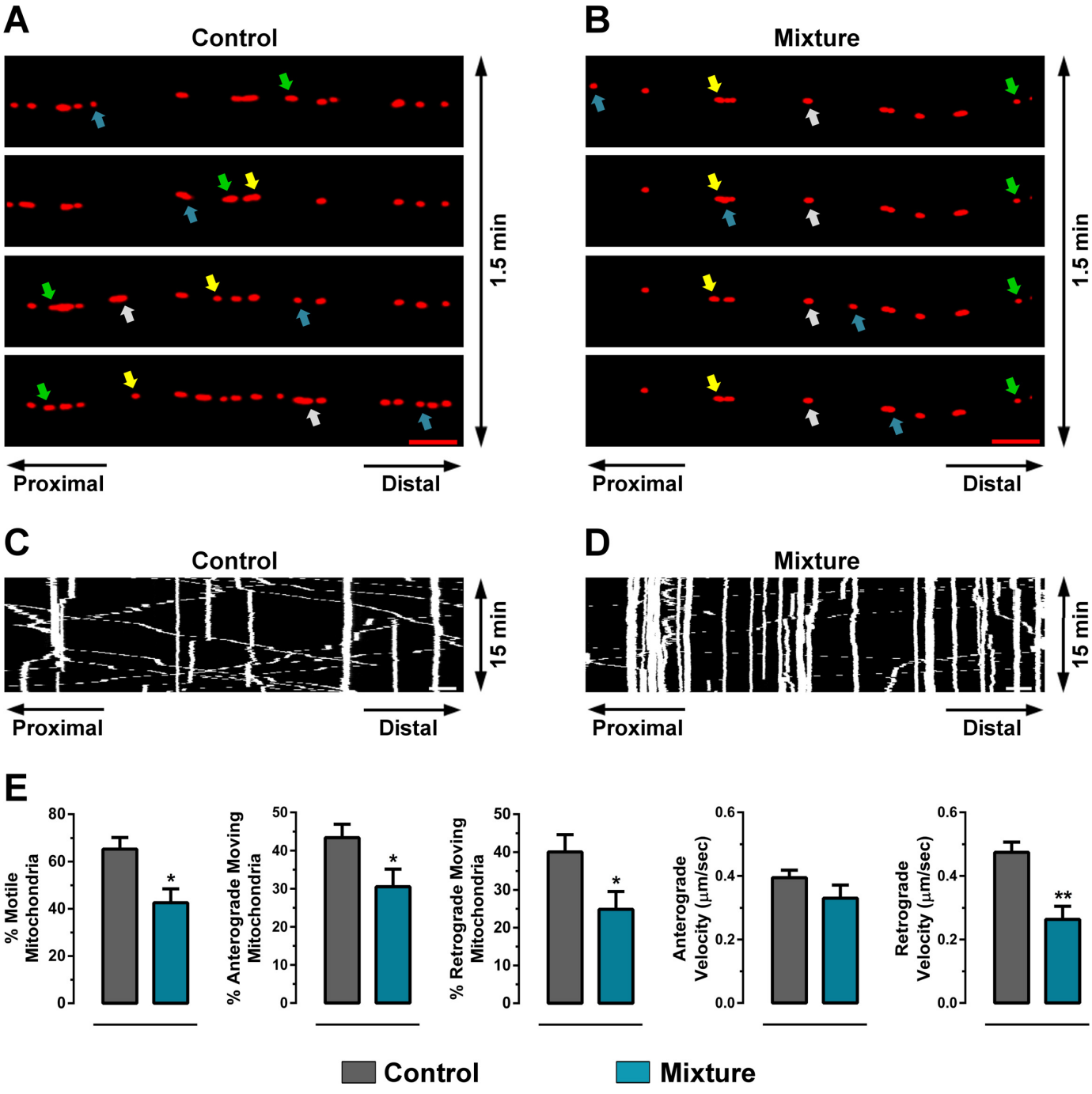

FIG. 2. Effect of the mixture of MDMA and its metabolites on axonal transport of mitochondria, in hippocampal neurons. Hippocampal neuronal cultures, transfected with MitDsRed and GFP, at 4DIV, were incubated with the mixture of MDMA and its metabolites α-MeDA, N-Me-α-MeDA, 5-(GSH)-α-MeDA, 5-(GSH)-N-Me-α-MeDA, 5-(NAC)-α-MeDA, and 5-(NAC)-N-Me-α-MeDA, each compound at 10μM, at 5DIV, and live-imaging of axonal transport of mitochondria was performed at 6DIV (24 h of exposure). (A and B) Series of four representative confocal images of live axons, taken every 30 s, of neurons overexpressing the mitochondrial-tagged protein MitDsRed, under control conditions (A) or after 24 h of exposure to the mixture of MDMA and its metabolites (B). Colored arrows identify the same mitochondria through the different acquisitions. Arrows to up and to down represent mitochondria that move in anterograde or retrograde directions, respectively. (C and D) Representative kymographs showing the full-time acquisition periods (15 min of movie) of control (C) or mixture-incubated hippocampal neurons (D), which show decreased mitochondrial movement. All kymographs are arranged with the distal axonal end to the right. (E) Graphical representation of the percentage of total motile mitochondria, motile mitochondria in anterograde or retrograde directions, and velocity in both anterograde and retrograde directions, as measured in kymographs. Data were analyzed using the Mann-Whitney's test and represent the mean ± SEM of 18–19 axons (neurons) per experimental group, from four independent experiments (*$p < 0.05$, **$p < 0.01$ mixture vs. control). Scale bar: 10 μm.

Downloaded from https://academic.oup.com/toxsci/article/139/2/407/2510934 by Consejo Superior de Investigaciones Cientificas (CSIC) user on 19 October 2021

not significantly changed (control = 0.394 ± 0.024 μm/s; mixture = 0.330 ± 0.042 μm/s), an impairment in retrograde velocity was observed (control = 0.474 ± 0.033 μm/s; mixture = 0.264 ± 0.041 μm/s, $p < 0.01$). Thus, these results indicate that the mixture of MDMA and its metabolites, at a range of concentrations with relevance to the *in vivo* scenario (Chu *et al.*, 1996; Erives *et al.*, 2008; Jones *et al.*, 2005), impaired axonal transport of mitochondria.

Tau Protein did not Play a Major Role on the Mitochondrial Trafficking Deficits Triggered by the Mixture of MDMA and its Metabolites

Previous studies have attributed an important role for Tau protein in regulating axonal transport of mitochondria (Kopeikina *et al.*, 2011; Llorens-Martín *et al.*, 2011; Shahpasand *et al.*, 2012; Vossel *et al.*, 2010), though anterograde and retrograde movements appear to be differently modulated (Dixit *et al.*, 2008). Furthermore, Tau protein function in regulating mitochondrial trafficking is critically dependent on its phosphorylation ratio (Llorens-Martín *et al.*, 2011; Shahpasand *et al.*, 2012). By using Tau (−/−) neurons (Fig. 3A) we studied the involvement of Tau protein on mitochondrial trafficking impairment associated with the mixture of MDMA and its metabolites. As shown in Figure 3, the lack of Tau protein significantly restored the deficits triggered by the mixture of MDMA and its metabolites in retrograde mitochondrial velocity. However, none of the remaining transport parameters evaluated were significantly modified, thus indicating a minor role for Tau protein on the reported trafficking phenotype.

Increased Fragmentation of Axonal Mitochondria was Linked to the Trafficking Deficits Triggered by the Mixture of MDMA and its Metabolites

Neurons are critically dependent on mitochondrial dynamics to ensure correct ATP supply and Ca^{2+} homeostasis (Sheng and Cai, 2012). Though a direct involvement of the profusion protein Mfn2 in regulating mitochondrial neuronal trafficking has been described (Misko *et al.*, 2010, 2012), the role of fission events on mitochondrial trafficking control has not been completely elucidated. However, despite this emerging relationship (Li *et al.*, 2004; Verstreken *et al.*, 2005), little is known regarding the response of mitochondrial fission/fusion to disease and stress. To confirm whether the mitochondrial trafficking deficits observed were associated with deregulation in mitochondrial fusion/fission events, we evaluated mitochondrial length on axonal extensions. Control mitochondria exhibited an average length of 0.555 ± 0.021 μm, whereas axonal mitochondria from neurons exposed to the mixture of MDMA and its metabolites were significantly shorter, with an average length of 0.429 ± 0.011 μm ($p < 0.0001$, Fig. 4A). Therefore, the impairment of mitochondrial movement induced by the mixture of MDMA and its metabolites was associated with increased fragmentation of axonal mitochondria.

Overexpression of Mitofusin2 or Drp1 K38A almost Completely Rescued the Mitochondrial Trafficking Deficits Triggered by the Mixture of MDMA and its Metabolites

Though a relationship between fusion proteins, namely Mfn2, and mitochondrial transport was recently described (Detmer and Chan, 2007; Misko *et al.*, 2010, 2012), whether the effect of Mfn2 on mitochondrial transport is related to its fusion properties is not completely established. Furthermore, the previous involvement of Drp1 in regulating mitochondrial density in dendrites (Li *et al.*, 2004) and axonal transport of mitochondria (Verstreken *et al.*, 2005) suggests that a deregulation of mitochondrial fusion/fission equilibrium, as observed by increased fragmentation of axonal mitochondria (Fig. 4A), may be related to the reported mitochondrial trafficking phenotype. As shown in Figures 4B–4D, overexpression of wild-type Mfn2 completely rescued the mitochondrial transport deficits elicited by the mixture of MDMA and its metabolites, when compared with Mfn2-nontransfected neurons. Similarly, overexpression of Drp1 K38A, a dominant negative construct that lacks fission properties (Zhao *et al.*, 2011), almost completely rescued the mixture-induced mitochondrial trafficking impairment, as compared with respective Drp1 K38A-nontransfected counterparts (Fig. 5). Thus, these findings indicate that proteins/mechanisms involved in mitochondrial fission/fusion may be disrupted by exposure to the mixture of MDMA and its metabolites, causing mitochondrial trafficking arrest in cultured hippocampal neurons.

CMT2A-Associated Mitofusin2 Mutant did not Rescue the Mitochondrial Trafficking Phenotype Induced by the Mixture of MDMA and its Metabolites

Charcot-Marie-Tooth's 2A disease, an autosomal dominant sensory-motor neuropathy, is associated with several mutations in Mfn2. One of these mutant forms is Mfn2 R94Q, which is characterized by impaired mitochondrial fusion properties (Detmer and Chan, 2007). Furthermore, this mutant protein is reported to produce a marked decrease in overall mitochondrial motility in axons of cultured sensory neurons (Baloh *et al.*, 2007) and altered mitochondrial distribution and transport along axons of dorsal root ganglion neurons (Misko *et al.*, 2010, 2012). Therefore, we transfected hippocampal neurons with Mfn2 R94Q to appraise the relative contribution of fission/fusion-dependent mechanisms in regulating the mitochondrial trafficking phenotype triggered by the mixture of MDMA and its metabolites. As shown in Figure 6, overexpression of Mfn2 R94Q did not modify the mixture-induced mitochondrial trafficking impairment, when compared with Mfn2 R94Q-nontransfected neurons. Thus, consistent with our experiments performed with wild-type Mfn2 and Drp1 K38A overexpressing neurons, these results indicate a critical dependence on mitochondrial fission/fusion-dependent mechanisms for the mitochondrial trafficking arrest caused by the mixture of MDMA and its metabolites.

Downloaded from https://academic.oup.com/toxsci/article/139/2/407/2510934 by Consejo Superior de Investigaciones Cientificas (CSIC) user on 19 October 2021

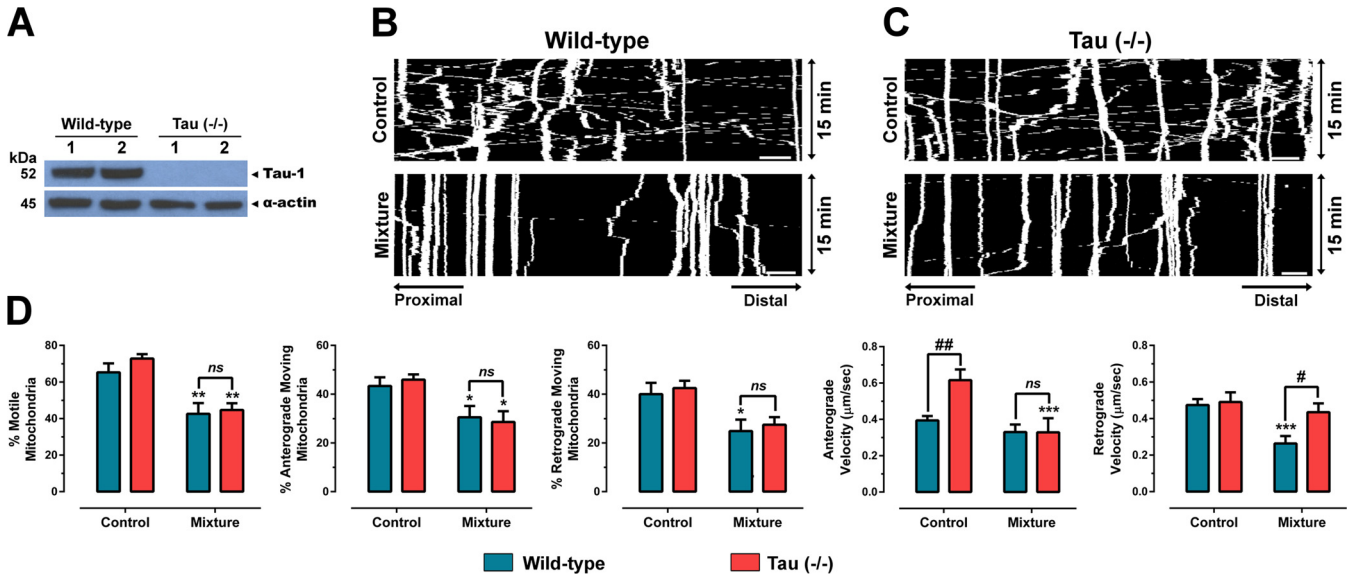

FIG. 3. Involvement of Tau protein on mitochondrial trafficking impairment induced by the mixture of MDMA and its metabolites. Experiments were performed in wild-type and Tau (−/−) hippocampal neurons. (A) Western blot analysis of Tau protein expression in wild-type and Tau (−/−) hippocampal neurons at 6DIV. Wild-type neurons express Tau protein, whereas it is not expressed in Tau (−/−) neurons (anti-Tau1 antibody, 1:50,000). Equal protein loading was confirmed with α-actin antibody (1:100,000). (B and D) Hippocampal neuronal cultures, transfected with MitDsRed and GFP at 4DIV, were exposed to the mixture of MDMA and its metabolites α-MeDA, N-Me-α-MeDA, 5-(GSH)-α-MeDA, 5-(GSH)-N-Me-α-MeDA, 5-(NAC)-α-MeDA, and 5-(NAC)-N-Me-α-MeDA, each compound at 10μM, at 5DIV, and live-imaging of axonal transport of mitochondria was performed at 6DIV (24 h of exposure). In (B) and (C), representative kymographs showing the full-time acquisition periods (15 min of movie) of wild-type (B) or Tau (−/−) hippocampal neurons (C), under control conditions or after 24 h of exposure to the mixture of MDMA and its metabolites, are presented. All kymographs are arranged with the distal axonal end to the right. In (D), the graphical representation of the percentage of total motile mitochondria, motile mitochondria in anterograde or retrograde directions, and velocity in both anterograde and retrograde directions, as in kymographs, are showed. Data were analyzed using two-way ANOVA, followed by Bonferroni's test for *post-hoc* evaluations, and represent the mean ± SEM of 10–19 axons (neurons) per experimental group, from at least three independent experiments [$^{*}p < 0.05$, $^{**}p < 0.01$, $^{***}p < 0.001$ mixture vs. control; $^{\#}p < 0.05$, $^{\#\#}p < 0.01$ Tau (−/−) vs. wild-type; *ns*: not significant]. Scale bar: 10 μm.

DISCUSSION

The present study clearly shows, for the first time, that the mixture of MDMA and its metabolites, at *in vivo* relevant concentrations, impaired axonal transport of mitochondria and increased mitochondrial fragmentation in cultured hippocampal neurons. Furthermore, by overexpressing wild-type or mutant proteins, mitochondrial fission/fusion-dependent mechanisms were implicated in the reported trafficking phenotype. Lastly, by using Tau (−/−) neurons, a minor role for Tau protein on the mixture-triggered mitochondrial trafficking impairment was revealed.

High energy demands and the requirement to maintain cellular homeostasis at sites distant to the cell body make neurons particularly vulnerable to mitochondrial dysfunction (Itoh *et al.*, 2013). Indeed, where extended arborization requires long-distance maneuvering of intracellular components, it has been suggested that disrupted mitochondrial translocation may contribute to the pathophysiology of neuronal injury (Deheshi *et al.*, 2013). Furthermore, there is emerging evidence suggesting that the damage of terminal axons may occur independently and by distinct mechanisms from those of cell bodies (Lee *et al.*, 2012). Importantly, selective damage to terminal axons is a characteristic marker of MDMA-associated neurotoxicity (Capela *et al.*, 2009).

In recent years, a more detailed picture has emerged about the cellular mechanisms ensuring mitochondrial integrity, and their relevance for neuronal degeneration. In the field of MDMA research, there is a general consensus that disruption of mitochondrial function likely contributes to pathological processes underlying MDMA's neurotoxicity (Alves *et al.*, 2007, 2009a,b; Puerta *et al.*, 2010; Quinton and Yamamoto, 2006). In fact, inhibition of mitochondrial respiratory complexes' proteins (Puerta *et al.*, 2010; Quinton and Yamamoto, 2006), oxidation of mitochondrial macromolecules (Alves *et al.*, 2007, 2009a,b) and deletions of mitochondrial DNA (Alves *et al.*, 2007, 2009a) have been associated with MDMA-induced neurotoxicity. Therefore, it is expected that mitochondrial dysfunction may be crucial in MDMA's neurotoxic effects.

Human studies have indicated that the memory and learning dysfunction in heavy MDMA users may be related to the drug's actions on hippocampus (Gouzoulis-Mayfrank *et al.*, 2003). Furthermore, animal studies have demonstrated the vulnerability of this brain area to MDMA's effects, including long-lasting memory deficits and deletions of mitochondrial DNA (Alves *et al.*, 2007, 2009a; Capela *et al.*, 2009). Altogether,

Downloaded from https://academic.oup.com/toxsci/article/139/2/407/2510934 by Consejo Superior de Investigaciones Cientificas (CSIC) user on 19 October 2021

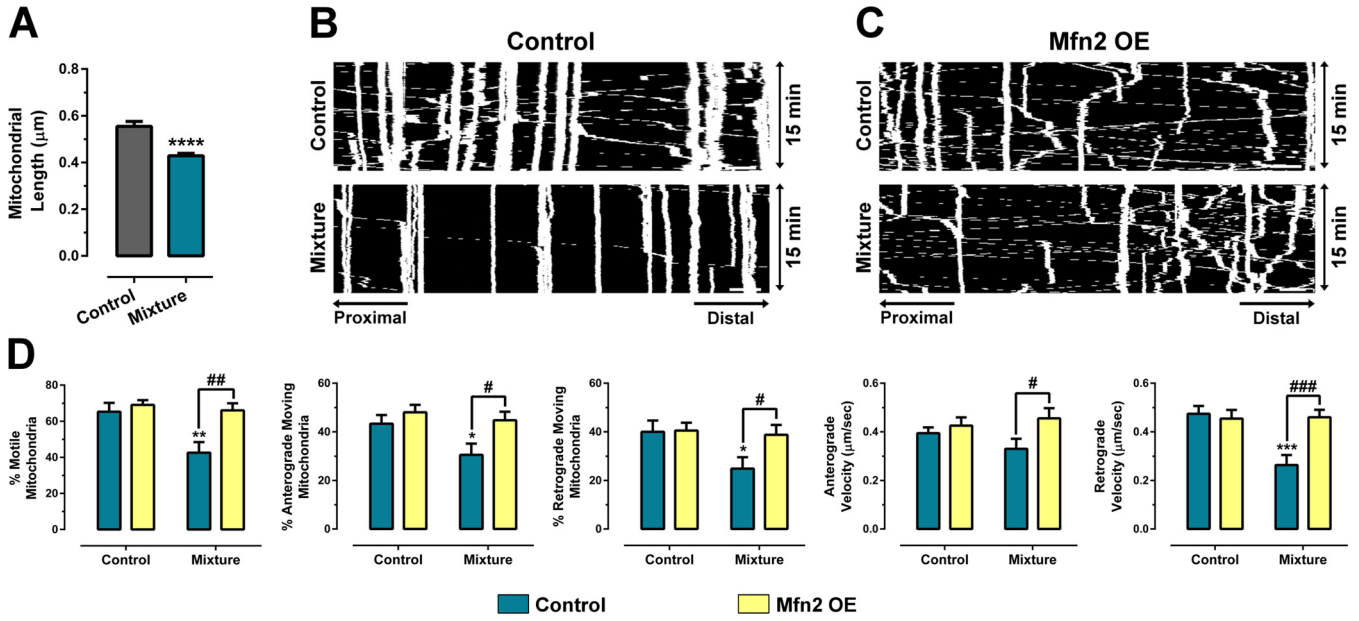

FIG. 4. Contribution of mitochondrial fission/fusion-dependent mechanisms for the mitochondrial trafficking impairment induced by the mixture of MDMA and its metabolites in hippocampal neurons. (A) Graphical representation of mitochondrial length, showing increased mitochondrial fragmentation following 24 h of exposure to the mixture of MDMA and its metabolites α-MeDA, N-Me-α-MeDA, 5-(GSH)-α-MeDA, 5-(GSH)-N-Me-α-MeDA, 5-(NAC)-α-MeDA, and 5-(NAC)-N-Me-α-MeDA, each compound at 10μM. Data represent mean ± SEM of 126–171 individual mitochondria (29–30 different axons) from three independent hippocampal cultures, and were analyzed using the Mann-Whitney's test (****$p < 0.0001$ mixture vs. control). (B and D) Effect of Mfn2 overexpression on mitochondrial trafficking impairment induced by the mixture of MDMA and its metabolites. Experiments were performed in control and Mfn2 overexpressing hippocampal neurons. Hippocampal neuronal cultures, transfected with MitDsRed and GFP or MitDsRed and GFP plus Mfn2 at 4DIV, were exposed to the mixture of MDMA and its metabolites, each compound at 10μM, at 5DIV, and live-imaging of axonal transport of mitochondria was performed at 6DIV (24 h of exposure). In (B) and (C), representative kymographs showing the full-time acquisition periods (15 min of movie) of control (B) or Mfn2 overexpressing neurons (C), under control conditions or after 24 h of exposure to the mixture of MDMA and its metabolites, are presented. All kymographs are arranged with the distal axonal end to the right. In (D), the graphical representation of the percentage of total motile mitochondria, motile mitochondria in anterograde or retrograde directions, and velocity in both anterograde and retrograde directions, as measured in kymographs, are showed. Data were analyzed using two-way ANOVA, followed by Bonferroni's test for *post-hoc* evaluations, and represent the mean ± SEM of 16–19 different axons (neurons) per experimental group, from four independent experiments (*$p < 0.05$, **$p < 0.01$, ***$p < 0.001$ mixture vs. control; $^{\#}p < 0.05$, $^{\#\#}p < 0.01$, $^{\#\#\#}p < 0.001$ Mfn2 overexpressing vs. control neurons). Scale bar: 10 μm.

these findings indicate a particular susceptibility of this brain area to MDMA's actions, thus rendering hippocampal cultures a relevant model to study MDMA-induced toxic effects at the mitochondrial level.

In accordance with previous studies, which have shown that MDMA and several of its metabolites coexist in the brain following peripheral administration of the drug (Chu *et al.*, 1996; Erives *et al.*, 2008; Jones *et al.*, 2005), we selected the MDMA metabolites α-MeDA, N-Me-α-MeDA, 5-(GSH)-α-MeDA, 5-(GSH)-N-Me-α-MeDA, 5-(NAC)-α-MeDA, and 5-(NAC)-N-Me-α-MeDA, to assess the effects of their mixture with MDMA on mitochondrial dynamics.

This study demonstrates, for the first time, that this mixture, at *in vivo* relevant concentrations, dramatically impaired mitochondrial trafficking along axons of cultured hippocampal neurons, as revealed by the reduced mitochondrial movement in anterograde and retrograde directions, as well as by a significant reduction in retrograde velocity. Considering the critical dependence of neurons on mitochondrial transport regarding proper energy supply and synaptic function (MacAskill and Kittler, 2010; Sheng and Cai, 2012), these results provide a new, and important, insight in the context of "ecstasy"-induced deleterious effects to the central nervous system. Additionally, these data suggest that alterations in neuronal mitochondrial trafficking may contribute to the acute- and long-lasting effects of MDMA in the brain.

A number of studies have suggested that increased expression or altered microtubule-binding of Tau may compromise axonal transport of mitochondria (Kopeikina *et al.*, 2011). However, other studies have described a Tau-independent regulation of axonal transport (Yuan *et al.*, 2008). Here, we showed that the trafficking impairment induced by the mixture of MDMA and its metabolites in Tau (−/−) neurons was comparable to the one found in wild-type neurons (only a partial rescue in retrograde velocity was found). In a previous study, we showed a partial dependence on Tau protein in MDMA-induced mitochondrial trafficking impairment, by exposing cultured hippocampal neurons to a high concentration of MDMA (Barbosa *et al.*, 2014c).

Downloaded from https://academic.oup.com/toxsci/article/139/2/407/2510934 by Consejo Superior de Investigaciones Cientificas (CSIC) user on 19 October 2021

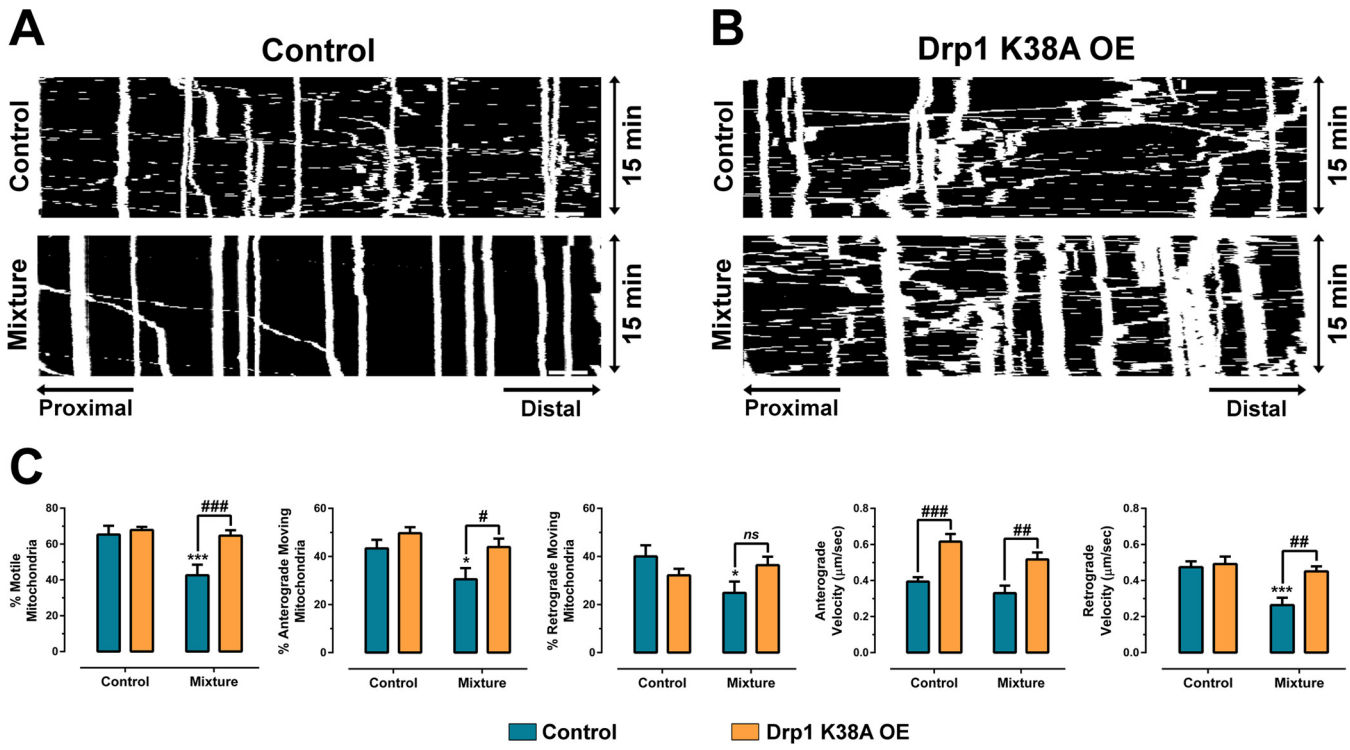

FIG. 5. Effect of Drp1 K38A overexpression on mitochondrial trafficking impairment induced by the mixture of MDMA and its metabolites. Experiments were performed in control and Drp1 K38A overexpressing hippocampal neurons. Hippocampal neuronal cultures, transfected with MitDsRed and GFP or MitDsRed and GFP plus Drp1 K38A at 4DIV, were exposed to the mixture of MDMA and its metabolites α-MeDA, N-Me-α-MeDA, 5-(GSH)-α-MeDA, 5-(GSH)-N-Me-α-MeDA, 5-(NAC)-α-MeDA, and 5-(NAC)-N-Me-α-MeDA, each compound at 10μM, at 5DIV, and live-imaging of axonal transport of mitochondria was performed at 6DIV (24 h of exposure). (A and B) Representative kymographs showing the full-time acquisition periods (15 min of movie) of control (A) or Drp1 K38A overexpressing neurons (B), under control conditions or after 24 h of exposure to the mixture of MDMA and its metabolites. All kymographs are arranged with the distal axonal end to the right. (C) Graphical representation of the percentage of total motile mitochondria, motile mitochondria in anterograde or retrograde directions, and velocity in both anterograde and retrograde directions, as measured in kymographs. Data were analyzed using two-way ANOVA, followed by Bonferroni's test for *post-hoc* evaluations, and represent the mean ± SEM of 18–19 different axons (neurons) per experimental group, from four independent experiments ($^{*}p < 0.05$, $^{***}p < 0.001$ mixture vs. control; $^{\#}p < 0.05$, $^{\#\#}p < 0.01$, $^{\#\#\#}p < 0.001$ Drp1 K38A overexpressing vs. control neurons; *ns*: not significant). Scale bar: 10 μm.

In this study, the minor dependence on Tau protein for the reported effect suggests that Tau-independent mechanisms are responsible for the mitochondrial trafficking arrest caused by a low concentration mixture of MDMA and its metabolites.

Fission events fragment mitochondria into smaller units, thus allowing mitochondrial transport to different subcellular localizations, such as nerve terminals (Itoh *et al.*, 2013). In this study, hippocampal neurons exposed to the mixture of MDMA and its metabolites presented mitochondria of reduced size, indicating increased mitochondrial fragmentation. Noteworthy, changes in mitochondrial morphology, resulting from excessive fission, have been associated with numerous neurodegenerative disorders (Rintoul and Reynolds, 2010; Wang *et al.*, 2013a) and neuronal injury (Frank *et al.*, 2001; Wang *et al.*, 2013a). Furthermore, oxidative stress, a common outcome in MDMA-related neuronal injury (Barbosa *et al.*, 2012, 2014a,b; Capela *et al.*, 2007, 2009), appears to modify mitochondrial response to fission events, resulting in increased mitochondrial fragmentation (Ghose *et al.*, 2013; Wang *et al.*, 2013b). In accordance, in a neuronal model of Parkinson's disease, the neuronal injury observed under oxidative stress conditions was prevented by chemical inhibition of mitochondrial fission (Qi *et al.*, 2012). Therefore, the increased mitochondrial fragmentation observed in this study suggests that the mixture of MDMA and its metabolites may alter mitochondrial fusion/fission equilibrium, a mitochondrial processing event, and, thus, contribute to the MDMA-induced neuronal dysfunction. However, though it is clear that mitochondrial fission plays a major role in restoring dysfunctional mitochondria and regulating mitochondrial transport (Verstreken *et al.*, 2005), whether mitochondrial dysfunction is the cause or a consequence of impaired mitochondrial transport remains unknown.

Like fission, mitochondrial fusion is also required for proper mitochondrial distribution in neurons (Baloh *et al.*, 2007; Misko *et al.*, 2010, 2012). Mfn2 appears to be critical in maintaining neuronal function and integrity, because its loss-of-function causes abnormal mitochondrial morphology, respiratory chain dysfunction and severe reduction of dopaminergic terminals in

Downloaded from https://academic.oup.com/toxsci/article/139/2/407/2510934 by Consejo Superior de Investigaciones Cientificas (CSIC) user on 19 October 2021

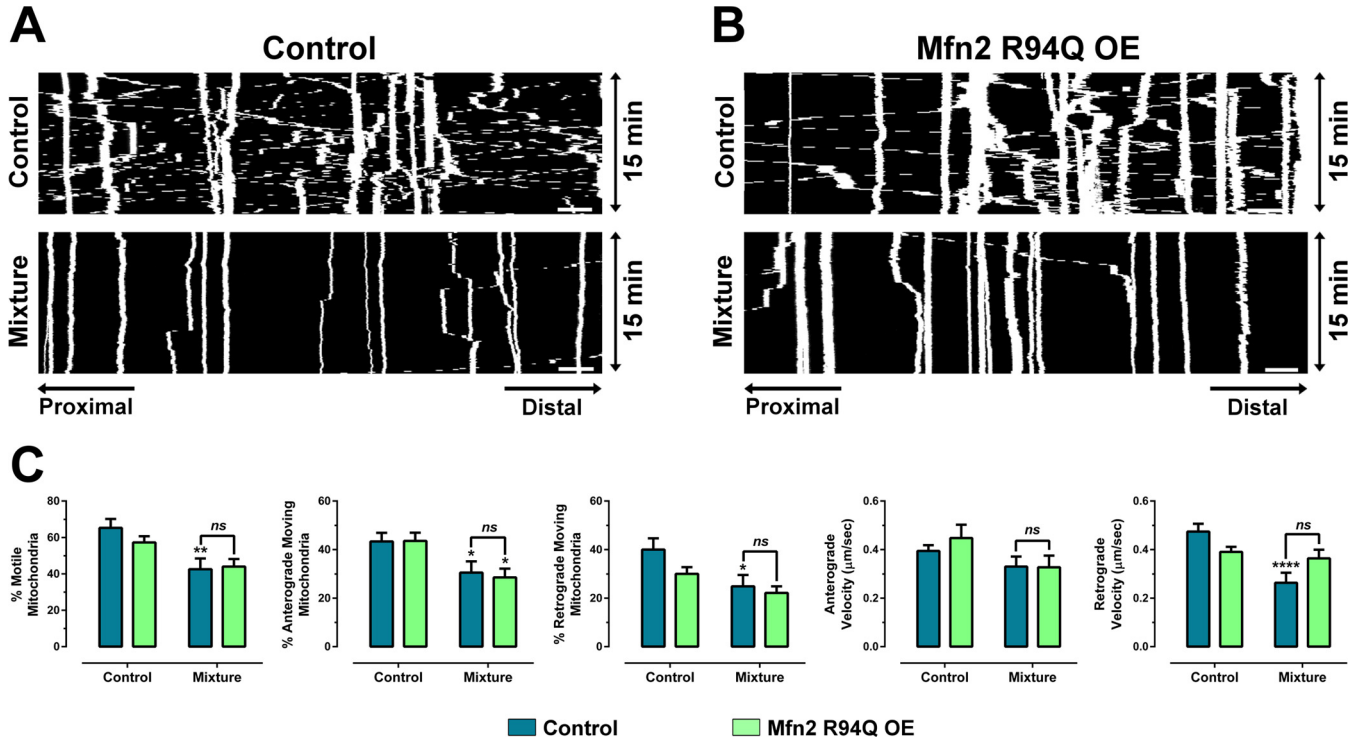

FIG. 6. Effect of Mfn2 R94Q overexpression on mitochondrial trafficking impairment induced by the mixture of MDMA and its metabolites. Experiments were performed in control and Mfn2 R94Q overexpressing hippocampal neurons. Hippocampal neuronal cultures, transfected with MitDsRed and GFP or MitDsRed and GFP plus Mfn2 R94Q at 4DIV, were exposed to the mixture of MDMA and its metabolites α-MeDA, N-Me-α-MeDA, 5-(GSH)-α-MeDA, 5-(GSH)-N-Me-α-MeDA, 5-(NAC)-α-MeDA, and 5-(NAC)-N-Me-α-MeDA, each compound at 10μM, at 5DIV, and live-imaging of axonal transport of mitochondria was performed at 6DIV (24 h of exposure). (A and B) Representative kymographs showing the full-time acquisition periods (15 min of movie) of control (A) or Mfn2 R94Q overexpressing neurons (B), under control conditions or after 24 h of exposure to the mixture of MDMA and its metabolites. All kymographs are arranged with the distal axonal end to the right. (C) Graphical representation of the percentage of total motile mitochondria, motile mitochondria in anterograde or retrograde directions, and velocity in both anterograde and retrograde directions, as measured in kymographs. Data were analyzed using two-way ANOVA, followed by Bonferroni's test for *post-hoc* evaluations, and represent the mean ± SEM of 18–19 different axons (neurons) per experimental group, from four independent experiments (*$p < 0.05$, **$p < 0.01$, ****$p < 0.0001$ mixture vs. control; *ns*: not significant). Scale bar: 10 μm.

mouse striatum (Lee *et al.*, 2012). In neurons, as in other cell types, the mutant fission protein Drp1 K38A, acting as a dominant negative, inhibits endogenous fission without affecting the normal activity of fusion proteins (Zhao *et al.*, 2011). In this study, it was demonstrated that the overexpression of Mfn2 or Drp1 K38A almost completely rescued the mixture-induced mitochondrial trafficking deficits, as compared with the respective Mfn2- or Drp1 K38A-nontransfected counterparts. However, Mfn2 overexpression was more effective than Drp1 K38A in preventing mitochondrial trafficking impairment. Additionally, in hippocampal neurons overexpressing the dominant negative Mfn2 mutant R94Q, a CMT2A mutant construct with impaired fusion (Detmer and Chan, 2007) and transport properties (Misko *et al.*, 2010, 2012), the mitochondrial trafficking impairment caused by the mixture of MDMA and its metabolites was not significantly changed, when compared with Mfn2 R94Q-nontransfected neurons. In control neurons, overexpression of Mfn2 or Mfn2 R94Q (with GFP and MitDsRed), did not significantly change any of the parameters assessed, compared with their nontransfected counterparts (only transfected with GFP and MitDsRed). Drp1 K38A overexpressing neurons (with GFP and MitDsRed) showed, however, higher anterograde velocity when compared with their respective nontransfected controls (only transfected with GFP and MitDsRed). These data indicate that fully functional Mfn2 was required to reverse the mixture-induced impaired mitochondrial trafficking. Additionally, because Mfn2 and Drp1 largely mitigated the mitochondrial trafficking deficits induced by the mixture of MDMA and its metabolites, these experiments also suggest that this mixture may alter the mitochondrial fusion/fission equilibrium, consistent with the reported increase in the fragmentation of axonal mitochondria.

The loss of synaptic terminals in MDMA-administrated rats is by far the most reported neurotoxic event associated with this drug of abuse (Capela *et al.*, 2009; Rudnick and Wall, 1992). Therefore, as neuronal mitochondrial trafficking and targeting to neuronal compartments and synapses are critical for many neuronal functions, including energy production and correct synaptic transmission (Barbosa *et al.*, 2014c; López-Doménech *et al.*, 2012; Sheng and Cai, 2012), we postulate

Downloaded from https://academic.oup.com/toxsci/article/139/2/407/2510934 by Consejo Superior de Investigaciones Cientificas (CSIC) user on 19 October 2021

that disrupted mitochondrial trafficking may contribute to the MDMA's neurotoxic and/or psychostimulant effects. Additionally, because alterations in mitochondrial morphology resulting from a failure of mitochondrial quality control mechanisms, like fusion/fission events, may ultimately result in a collapse of mitochondrial network and neuronal injury (Rugarli and Langer, 2012), these data describe a potential new mechanism underlying the effects of MDMA and its metabolites at the neuronal level. Lastly, with the experimental approach introduced in this study, in which low micromolar concentrations of MDMA and its main *in vivo* metabolites were combined in a mixture, thus becoming more representative of the *in vivo* scenario, these data provide a new breakthrough in the field of MDMA research, which may help in clarifying the mechanisms involved in MDMA-induced neuronal dysfunction, degeneration, and neurotoxicity.

SUPPLEMENTARY DATA

Supplementary data are available online at http://toxsci.oxfordjournals.org/.

FUNDING

Ministerio de Ciencia e Innovacion (MICINN), Spain (BFU2008-3980); Plan Nacional de Drogas, Spain; Fundação para a Ciência e a Tecnologia (FCT), Portugal (Project PTDC/SAU-FCF/102958/2008) under the framework of Programa Operacional Temático Factores de Competitividade (COMPTE) do Quadro Comunitário de Apoio III and Fundo Comunitário Europeu (FEDER) (FCOMP-01-0124-FEDER-011079); FCT, Portugal (SFRH/BD/64939/2009 to D.J.B.); FCT, Portugal (RECI/BBB-BQB/0230/2012).

ACKNOWLEDGMENT

We thank Luca Scorrano (University of Geneva) and Miquel Vila (VHIR, Barcelona) for providing the Mitofusin and Drp1 constructs. DJB greatly acknowledge to Renata Silva PhD for the stimulant comments.

REFERENCES

Alves, E., Binienda, Z., Carvalho, F., Alves, C. J., Fernandes, E., de Lourdes Bastos, M., Tavares, M. A., and Summavielle, T. (2009a). Acetyl-l-carnitine provides effective *in vivo* neuroprotection over 3,4-methylenedioximethamphetamine-induced mitochondrial neurotoxicity in the adolescent rat brain. *Neuroscience* **158**, 514–523.

Alves, E., Summavielle, T., Alves, C. J., Custódio, J. B., Fernandes, E., Lourdes Bastos, M., Tavares, M. A., and Carvalho, F. (2009b). Ecstasy-induced oxidative stress to adolescent rat brain mitochondria *in vivo*: Influence of monoamine oxidase type A. *Addict. Biol.* **14**, 185–193.

Alves, E., Summavielle, T., Alves, C. J., Gomes-da-Silva, J., Barata, J. C., Fernandes, E., Bastos, M. d. L., Tavares, M. A., and Carvalho, F. (2007). Monoamine oxidase-B mediates ecstasy-induced neurotoxic effects to adolescent rat brain mitochondria. *J. Neurosci.* **27**, 10203–10210.

Bai, F., Jones, D. C., Lau, S. S., and Monks, T. J. (2001). Serotonergic neurotoxicity of 3,4-(±)-methylenedioxyamphetamine and 3,4-(±)-methylendioxymethamphetamine (ecstasy) is potentiated by inhibition of γ-glutamyl transpeptidase. *Chem. Res. Toxicol.* **14**, 863–870.

Baloh, R. H., Schmidt, R. E., Pestronk, A., and Milbrandt, J. (2007). Altered axonal mitochondrial transport in the pathogenesis of Charcot-Marie-Tooth disease from mitofusin 2 mutations. *J. Neurosci.* **27**, 422–430.

Barbosa, D. J., Capela, J. P., Oliveira, J. M. A., Silva, R., Ferreira, L. M., Siopa, F., Branco, P. S., Fernandes, E., Duarte, J. A., de Lourdes Bastos, M., *et al.* (2012). Pro-oxidant effects of Ecstasy and its metabolites in mouse brain synaptosomes. *Br. J. Pharmacol.* **165**, 1017–1033.

Barbosa, D. J., Capela, J. P., Silva, R., Ferreira, L. M., Branco, P. S., Fernandes, E., Bastos, M. L., and Carvalho, F. (2014a). "Ecstasy"-induced toxicity in SH-SY5Y differentiated cells: Role of hyperthermia and metabolites. *Arch. Toxicol.* **88**, 515–531.

Barbosa, D. J., Capela, J. P., Silva, R., Vilas-Boas, V., Ferreira, L. M., Branco, P. S., Fernandes, E., Bastos, M. L., and Carvalho, F. (2014b). The mixture of "ecstasy" and its metabolites is toxic to human SH-SY5Y differentiated cells at *in vivo* relevant concentrations. *Arch. Toxicol.* **88**, 455–473.

Barbosa, D. J., Serrat, R., Mirra, S., Quevedo, M., Gómez de Barreda, E., Ávila, J., Fernandes, E., Bastos, M. L., Capela, J. P., Carvalho, F., *et al.* (2014c). MDMA impairs mitochondrial neuronal trafficking in a Tau- and Mitofusin2/Drp1-dependent manner. *Arch. Toxicol.* doi: 10.1007/s00204-014-1209-7, [Epub ahead of print].

Baumann, M. H., Zolkowska, D., Kim, I., Scheidweiler, K. B., Rothman, R. B., and Huestis, M. A. (2009). Effects of dose and route of administration on pharmacokinetics of (±)-3,4-methylenedioxymethamphetamine in the rat. *Drug Metab. Dispos.* **37**, 2163–2170.

Busceti, C. L., Biagioni, F., Riozzi, B., Battaglia, G., Storto, M., Cinque, C., Molinaro, G., Gradini, R., Caricasole, A., Canudas, A. M., *et al.* (2008). Enhanced tau phosphorylation in the hippocampus of mice treated with 3,4-methylenedioxymethamphetamine ("ecstasy"). *J. Neurosci.* **28**, 3234–3245.

Capela, J. P., Carmo, H., Remião, F., Bastos, M. L., Meisel, A., and Carvalho, F. (2009). Molecular and cellular mechanisms of ecstasy-induced neurotoxicity: An overview. *Mol. Neurobiol.* **39**, 210–271.

Capela, J. P., Macedo, C., Branco, P. S., Ferreira, L. M., Lobo, A. M., Fernandes, E., Remião, F., Bastos, M. L., Dirnagl, U., Meisel, A., *et al.* (2007). Neurotoxicity mechanisms of thioether ecstasy metabolites. *Neuroscience* **146**, 1743–1757.

Capela, J. P., Meisel, A., Abreu, A. R., Branco, P. S., Ferreira, L. M., Lobo, A. M., Remião, F., Bastos, M. L., and Carvalho, F. (2006). Neurotoxicity of ecstasy metabolites in rat cortical neurons, and influence of hyperthermia. *J. Pharmacol. Exp. Ther.* **316**, 53–61.

Carvalho, M., Carmo, H., Costa, V. M., Capela, J. P., Pontes, H., Remião, F., Carvalho, F., and Bastos, M. L. (2012). Toxicity of amphetamines: An update. *Arch. Toxicol.* **86**, 1167–1231.

Cereghetti, G. M., Stangherlin, A., de Brito, O. M., Chang, C. R., Blackstone, C., Bernardi, P., and Scorrano, L. (2008). Dephosphorylation by calcineurin regulates translocation of Drp1 to mitochondria. *Proc. Natl. Acad. Sci. U.S.A.* **105**, 15803–15808.

Chu, T., Kumagai, Y., DiStefano, E. W., and Cho, A. K. (1996). Disposition of methylenedioxymethamphetamine and three metabolites in the brains of different rat strains and their possible roles in acute serotonin depletion. *Biochem. Pharmacol.* **51**, 789–796.

Concheiro, M., Baumann, M. H., Scheidweiler, K. B., Rothman, R. B., Marrone, G. F., and Huestis, M. A. (2014). Nonlinear pharmacokinetics of (±)3,4-

Downloaded from https://academic.oup.com/toxsci/article/139/2/407/2510934 by Consejo Superior de Investigaciones Cientificas (CSIC) user on 19 October 2021

methylenedioxymethamphetamine (MDMA) and its pharmacodynamic consequences in the rat. *Drug Metab. Dispos.* **42**, 119–125.

De La Torre, R., Farré, M., Ortuño, J., Mas, M., Brenneisen, R., Roset, P. N., Segura, J., and Camí, J. (2000). Non-linear pharmacokinetics of MDMA ('ecstasy') in humans. *Br. J. Clin. Pharmacol.* **49**, 104–109.

Deheshi, S., Pasqualotto, B. A., and Rintoul, G. L. (2013). Mitochondrial trafficking in neuropsychiatric diseases. *Neurobiol. Dis.* **51**, 66–71.

Delaforge, M., Jaouen, M., and Bouille, G. (1999). Inhibitory metabolite complex formation of methylenedioxymethamphetamine with rat and human cytochrome P450. Particular involvement of CYP 2D. *Environ. Toxicol. Pharmacol.* **7**, 153–158.

Detmer, S. A., and Chan, D. C. (2007). Complementation between mouse Mfn1 and Mfn2 protects mitochondrial fusion defects caused by CMT2A disease mutations. *J. Cell Biol.* **176**, 405–414.

Dixit, R., Ross, J. L., Goldman, Y. E., and Holzbaur, E. L. F. (2008). Differential regulation of dynein and kinesin motor proteins by tau. *Science* **319**, 1086–1089.

Erives, G. V., Lau, S. S., and Monks, T. J. (2008). Accumulation of neurotoxic thioether metabolites of 3,4-(±)-methylenedioxymethamphetamine in rat brain. *J. Pharmacol. Exp. Ther.* **324**, 284–291.

Esteban, B., O'Shea, E., Camarero, J., Sanchez, V., Green, A. R., and Colado, M. I. (2001). 3,4-Methylenedioxymethamphetamine induces monoamine release, but not toxicity, when administered centrally at a concentration occurring following a peripherally injected neurotoxic dose. *Psychopharmacology* **154**, 251–260.

Ferguson, C. S., and Tyndale, R. F. (2011). Cytochrome P450 enzymes in the brain: Emerging evidence of biological significance. *Trends Pharmacol. Sci.* **32**, 708–714.

Frank, S., Gaume, B., Bergmann-Leitner, E. S., Leitner, W. W., Robert, E. G., Catez, F., Smith, C. L., and Youle, R. J. (2001). The role of dynamin-related protein 1, a mediator of mitochondrial fission, in apoptosis. *Dev. Cell* **1**, 515–525.

Ghose, P., Park, E. C., Tabakin, A., Salazar-Vasquez, N., and Rongo, C. (2013). Anoxia-reoxygenation regulates mitochondrial dynamics through the hypoxia response pathway, SKN-1/Nrf, and stomatin-like protein STL-1/SLP-2. *PLoS Genet.* **9**, e1004063.

Gollamudi, R., Ali, S. F., Lipe, G., Newport, G., Webb, P., Lopez, M., Leakey, J. E., Kolta, M., and Slikker, W. J. (1989). Influence of inducers and inhibitors on the metabolism *in vitro* and neurochemical effects *in vivo* of MDMA. *Neurotoxicology* **10**, 455–466.

Gouzoulis-Mayfrank, E., Thimm, B., Rezk, M., Hensen, G., and Daumann, J. (2003). Memory impairment suggests hippocampal dysfunction in abstinent ecstasy users. *Prog. Neuropsychopharmacol. Biol. Psychiatry* **27**, 819–827.

Granado, N., Ares-Santos, S., Oliva, I., O´Shea, E., Martin, E. D., Colado, M. I., and Moratalla, R. (2011). Dopamine D2-receptor knockout mice are protected against dopaminergic neurotoxicity induced by methamphetamine or MDMA. *Neurobiol. Dis.* **42**, 391–403.

Heydari, A., Yeo, K. R., Lennard, M. S., Ellis, S. W., Tucker, G. T., and Rostami-Hodjegan, A. (2004). Mechanism-based inactivation of CYP2D6 by methylenedioxymethamphetamine. *Drug Metab. Dispos.* **32**, 1213–1217.

Itoh, K., Nakamura, K., Iijima, M., and Sesaki, H. (2013). Mitochondrial dynamics in neurodegeneration. *Trends Cell Biol.* **23**, 64–71.

Jones, D. C., Duvauchelle, C., Ikegami, A., Olsen, C. M., Lau, S. S., de la Torre, R., and Monks, T. J. (2005). Serotonergic neurotoxic metabolites of ecstasy identified in rat brain. *J. Pharmacol. Exp. Ther.* **313**, 422–431.

Kopeikina, K. J., Carlson, G. A., Pitstick, R., Ludvigson, A. E., Peters, A., Luebke, J. I., Koffie, R. M., Frosch, M. P., Hyman, B. T., and Spires-Jones, T. L. (2011). Tau accumulation causes mitochondrial distribution deficits in neurons in a mouse model of tauopathy and in human alzheimer's disease grain. *Am. J. Pathol.* **179**, 2071–2082.

Lee, S., Sterky, F. H., Mourier, A., Terzioglu, M., Cullheim, S., Olson, L., and Larsson, N. (2012). Mitofusin 2 is necessary for striatal axonal projections of midbrain dopamine neurons. *Hum. Mol. Genet.* **21**, 4827–4835.

Li, Z., Okamoto, K., Hayashi, Y., and Sheng, M. (2004). The importance of dendritic mitochondria in the morphogenesis and plasticity of spines and synapses. *Cell* **119**, 873–887.

Llorens-Martín, M., López-Doménech, G., Soriano, E., and Avila, J. (2011). GSK3β is involved in the relief of mitochondria pausing in a tau-dependent manner. *PLoS One* **6**, e27686.

López-Doménech, G., Serrat, R., Mirra, S., D'Aniello, S., Somorjai, I., Abad, A., Vitureira, N., García-Arumí, E., Alonso, M. T., Rodriguez-Prados, M., *et al.* (2012). The Eutherian Armcx genes regulate mitochondrial trafficking in neurons and interact with Miro and Trak2. *Nat. Commun.* **3**, 814.

MacAskill, A. F., and Kittler, J. T. (2010). Control of mitochondrial transport and localization in neurons. *Trends Cell Biol.* **20**, 102–112.

Macaskill, A. F., Rinholm, J. E., Twelvetrees, A. E., Arancibia-Carcamo, I. L., Muir, J., Fransson, A., Aspenstrom, P., Attwell, D., and Kittler, J. T. (2009). Miro1 is a calcium sensor for glutamate receptor-dependent localization of mitochondria at synapses. *Neuron* **61**, 541–555.

Misko, A., Jiang, S., Wegorzewska, I., Milbrandt, J., and Baloh, R. H. (2010). Mitofusin 2 is necessary for transport of axonal mitochondria and interacts with the Miro/Milton complex. *J. Neurosci.* **30**, 4232–4240.

Misko, A. L., Sasaki, Y., Tuck, E., Milbrandt, J., and Baloh, R. H. (2012). Mitofusin2 mutations disrupt axonal mitochondrial positioning and promote axon degeneration. *J. Neurosci.* **32**, 4145–4155.

Mueller, M., Yuan, J., Felim, A., Neudörffer, A., Peters, F. T., Maurer, H. H., McCann, U. D., Largeron, M., and Ricaurte, G. A. (2009). Further studies on the role of metabolites in (±)-3,4-methylenedioxymethamphetamine-induced serotonergic neurotoxicity. *Drug Metab. Dispos.* **37**, 2079–2086.

Parrott, A. C. (2012). MDMA and 5-HT neurotoxicity: The empirical evidence for its adverse effects in humans – no need for translation. *Br. J. Pharmacol.* **166**, 1518–1520.

Pizarro, N., Farre, M., Pujadas, M., Peiro, A. M., Roset, P. N., Joglar, J., and de la Torre, R. (2004). Stereochemical analysis of 3,4-methylenedioxymethamphetamine and its main metabolites in human samples including the catechol-type metabolite (3,4-dihydroxymethamphetamine). *Drug Metab. Dispos.* **32**, 1001–1007.

Puerta, E., Hervias, I., Goñi-Allo, B., Zhang, S. F., Jordán, J., Starkov, A. A., and Aguirre, N. (2010). Methylenedioxymethamphetamine inhibits mitochondrial complex I activity in mice: A possible mechanism underlying neurotoxicity. *Br. J. Pharmacol.* **160**, 233–245.

Qi, X., Qvit, N., Su, Y., and Mochly-Rosen, D. (2012). Novel Drp1 inhibitor diminishes aberrant mitochondrial fission and neurotoxicity. *J. Cell Sci.* **126**, 789–802.

Quinton, M. S., and Yamamoto, B. K. (2006). Causes and consequences of methamphetamine and MDMA toxicity. *AAPS J.* **8**, 337–347.

Research, I. f. L. A. (2011). *Guide for the Care and Use of Laboratory Animals*. 8th ed., The National Academies Press, Washington, DC, USA.

Rintoul, G. L., and Reynolds, I. J. (2010). Mitochondrial trafficking and morphology in neuronal injury. *Biochim. Biophys. Acta* **1802**, 143–150.

Roberts, G. M. P., Nestor, L., and Garavan, H. (2009). Learning and memory deficits in ecstasy users and their neural correlates during a face-learning task. *Brain Res.* **1292**, 71–81.

Rudnick, G., and Wall, S. C. (1992). The molecular mechanism of "ecstasy" [3,4-methylenedioxy-methamphetamine (MDMA)]: Serotonin transporters are targets for MDMA-induced serotonin release. *Proc. Natl. Acad. Sci. U.S.A.* **89**, 1817–1821.

Rugarli, E. I., and Langer, T. (2012). Mitochondrial quality control: A matter of life and death for neurons. *EMBO J.* **31**, 1336–1349.

Downloaded from https://academic.oup.com/toxsci/article/139/2/407/2510934 by Consejo Superior de Investigaciones Cientificas (CSIC) user on 19 October 2021

Russo, G. J., Louie, K., Wellington, A., Macleod, G. T., Hu, F., Panchumarthi, S., and Zinsmaier, K. E. (2009). Drosophila miro is required for both anterograde and retrograde axonal mitochondrial transport. *J. Neurosci.* **29**, 5443–5455.

Segura, M., Ortuño, J., Farré, M., McLure, J. A., Pujadas, M., Pizarro, N., Llebaria, A., Joglar, J., Roset, P. N., Segura, J. , *et al.* (2001). 3,4-Dihydroxymethamphetamine (HHMA). A major *in vivo* 3,4-methylenedioxymethamphetamine (MDMA) metabolite in humans. *Chem. Res. Toxicol.* **14**, 1203–1208.

Shahpasand, K., Uemura, I., Saito, T., Asano, T., Hata, K., Shibata, K., Toyoshima, Y., Hasegawa, M., and Hisanaga, S. (2012). Regulation of mitochondrial transport and inter-microtubule spacing by tau phosphorylation at the sites hyperphosphorylated in alzheimer's disease. *J. Neurosci.* **32**, 2430–2441.

Sheng, Z., and Cai, Q. (2012). Mitochondrial transport in neurons: Impact on synaptic homeostasis and neurodegeneration. *Nat. Rev. Neurosci.* **13**, 77–93.

Song, Z., Ghochani, M., McCaffery, J. M., Frey, T. G., and Chan, D. C. (2009). Mitofusins and OPA1 mediate sequential steps in mitochondrial membrane fusion. *Mol. Biol. Cell* **20**, 3525–3532.

Tai, Y. F., Hoshi, R., Brignell, C. M., Cohen, L., Brooks, D. J., Curran, H. V., and Piccini, P. (2011). Persistent nigrostriatal dopaminergic abnormalities in ex-users of MDMA ("Ecstasy"): An 18F-dopa PET study. *Neuropsychopharmacology* **36**, 735–743.

Verstreken, P., Ly, C. V., Venken, K. J. T., Koh, T., Zhou, Y., and Bellen, H. J. (2005). Synaptic mitochondria are critical for mobilization of reserve pool vesicles at drosophila neuromuscular junctions. *Neuron* **47**, 365–378.

Vossel, K. A., Zhang, K., Brodbeck, J., Daub, A. C., Sharma, P., Finkbeiner, S., Cui, B., and Mucke, L. (2010). Tau reduction prevents Aβ-induced defects in axonal transport. *Science* **330**, 198.

Wang, D. B., Garden, G. A., Kinoshita, C., Wyles, C., Babazadeh, N., Sopher, B., Kinoshita, Y., and Morrison, R. S. (2013a). Declines in Drp1 and Parkin expression underlie DNA damage-induced changes in mitochondrial length and neuronal death. *J. Neurosci.* **33**, 1357–1365.

Wang, X., and Schwarz, T. L. (2009). The mechanism of Ca^{2+}-dependent regulation of kinesin-mediated mitochondrial motility. *Cell* **136**, 163–174.

Wang, X., Wang, W., Li, L., Perry, G., Lee, H. G., and Zhu, X. (2013b). Oxidative stress and mitochondrial dysfunction in Alzheimer's disease. *Biochim. Biophys. Acta* doi: 10.1016/j.bbadis.2013.10.015, [Epub ahead of print].

Yuan, A., Kumar, A., Peterhoff, C., Duff, K., and Nixon, R. A. (2008). Axonal transport rates *in vivo* are unaffected by tau deletion or overexpression in mice. *J. Neurosci.* **28**, 1682–1687.

Zhao, J., Liu, T., Jin, S., Wang, X., Qu, M., Uhlen, P., Tomilin, N., Shupliakov, O., Lendahl, U., and Nister, M. (2011). Human MIEF1 recruits Drp1 to mitochondrial outer membranes and promotes mitochondrial fusion rather than fission. *EMBO J.* **30**, 2762–2778.

Downloaded from https://academic.oup.com/toxsci/article/139/2/407/2510934 by Consejo Superior de Investigaciones Cientificas (CSIC) user on 19 October 2021